Magneto-optical properties and charge-spin coupling in the molecular $(2,3\text{-dmpyH})_2CuBr_4$ spin-ladder material

J. L. White,[1] C. Lee,[2] Ö. Günaydin-Şen,[3] L. C. Tung,[4] H. M. Christen,[5] Y. J. Wang,[4] M. M. Turnbull,[6] C. P. Landee,[7] R. D. McDonald,[8] S. A. Crooker,[8] J. Singleton,[8] M.-H. Whangbo,[2] and J. L. Musfeldt[3]

[1]*Department of Physics, University of Tennessee, Knoxville, Tennessee 37996, USA*

[2]*Department of Chemistry, North Carolina State University, Raleigh, North Carolina 27695, USA*

[3]*Department of Chemistry, University of Tennessee, Knoxville, Tennessee 37996, USA*

[4]*National High Magnetic Field Laboratory, Tallahassee, Florida 32310, USA*

[5]*Materials Science and Technology Division, Oak Ridge National Laboratory, Oak Ridge, Tennessee 37831, USA*

[6]*Department of Chemistry, Clark University, Worcester, Massachusetts 01610, USA*

[7]*Department of Physics, Clark University, Worcester, Massachusetts 01610, USA*

[8]*National High Magnetic Field Laboratory, Los Alamos National Laboratory, Los Alamos, New Mexico 87545, USA*

(Received 1 November 2009; revised manuscript received 19 January 2010; published 26 February 2010)

We investigated the magnetic and optical properties of $(2,3\text{-dmpyH})_2CuBr_4$, an unusual antiferromagnetic quantum spin ladder with strong rail interactions that can be saturated in a 30 T field. This transition drives a field-induced color change, a dramatic example of charge-spin coupling in a molecular material. Spin-density calculations reveal that electronic structure is sensitive to the magnetic state because magnetic orbital character depends on the spin arrangement between adjacent $CuBr_4^{2-}$ chromophores. This finding suggests that molecular architecture and the magnetic arrangement between molecular units might be used to control magnetochromism.

DOI: 10.1103/PhysRevB.81.052407 PACS number(s): 78.20.Ls, 75.30.Et, 75.50.Ee, 78.20.Ci

Quantum spin ladders are important materials for fundamental investigations of quantum criticality and as physical manifestations of coupled spin chains. Although many of the best-studied systems are based on copper-oxide chemistry,[1–3] molecule-based materials offer important advantages including smaller exchange interactions, molecular-level tunability, and architectural control.[4,5] The former makes molecular ladders easier to saturate with conventional powered and pulsed magnets. A complementary strategy for reducing magnetic energy scales is to employ weak-field ligands (i.e., substitution of halide for oxide).[5–18] We take advantage of both techniques to investigate an important consequence of charge-spin coupling in ladders: magnetic field-induced color change. Like photoinduced magnetism,[19,20] magnetochromism has its origins in charge-spin coupling but uses a magnetic field to tune electronic structure rather than light to modify the magnetic state.

Bis(2,3-dimethylpyridinium) tetrabromocuprate $[(2,3\text{-dmpyH})_2CuBr_4]$ is a molecular material comprised of $CuBr_4^{2-}$ anions that carry spin and act as chromophores and organic counterions that control orientation, packing, and charge balance.[6] The characteristic ladderlike structure (inset, Fig. 1) consists of rungs and rails formed by single Br···Br contacts with the rungs related via an inversion center and the rails related by unit-cell translations.[6] Bulk magnetic property measurements indicate $J_{\parallel}=-16.8$ K and $J_{\perp}=-8.68$ K, yielding a $J_{\perp}/J_{\parallel}$ ratio of 0.52.[6] Here, we employ a spin Hamiltonian of $-\Sigma J_{ij}S_iS_j$, where $J_{\parallel}$ and $J_{\perp}$ are the exchange interactions along the rails and rungs, respectively. This system is (i) a rare example of a ladder with strong rail interactions and (ii) in the theoretically interesting intermediate coupling regime. Both factors differentiate it from more common strong-rung materials. Inelastic neutron scattering confirms two-leg spin-ladder character.[21]

In order to investigate the interplay between charge, structure, and magnetism in a tunable molecule-based spin ladder, we measured the magnetic and optical properties of $(2,3\text{-dmpyH})_2CuBr_4$. Despite the difference between magnetic and electronic energy scales, coupling between the spin and charge channels gives rise to a field-induced color change that strikingly tracks the magnetization. Spin-density calculations reveal that the spin arrangement between adjacent $CuBr_4^{2-}$ chromophores controls the orbital character in the low- and high-field states, a mechanism that can be used (along with crystal architecture) to control color and color change in other magnetic materials.

Single crystals of $(2,3\text{-dmpyH})_2CuBr_4$ were grown by solution techniques as described previously.[6,22] Single-crystal magnetization was measured using a hand-wound pickup coil and 50 T short and midpulse magnets.[13] Data were taken at 4.0 K, 1.6 K, and 480 mK. The absolute magnetization was determined via comparison with low-field calibrated susceptibility data. Transmittance measurements were performed on both single-crystal and isotropic pressed pellet samples[22] using a series of spectrometers covering a wide range of energy (74 meV–6.5 eV), temperature (1.5–300 K), and magnetic field (0–53 T). Transmittance was related to absorption as $\alpha(E)=-\frac{1}{hd}\ln[\mathcal{T}(E)]$, where h is loading fraction, d is thickness, and $\mathcal{T}(E)$ is the transmittance. Energy-dependent magneto-optical spectroscopies of the isotropic sample were carried out using a 60 T long-pulse magnet at 1.5 K. The data were used in combination with $\alpha(E)$ to back-calculate $\alpha(E,H)$. Absorption differences, which highlight field-induced spectral changes, were calculated as $\alpha(E,H)-\alpha(E,0)$, where $\alpha(E,H)$ is the absorption in magnetic field and $\alpha(E,0)$ is the zero-field absorption. The absolute value of the absorption difference was integrated between 1.78 and 2.85 eV (over the range of the magneto-optical effects), to

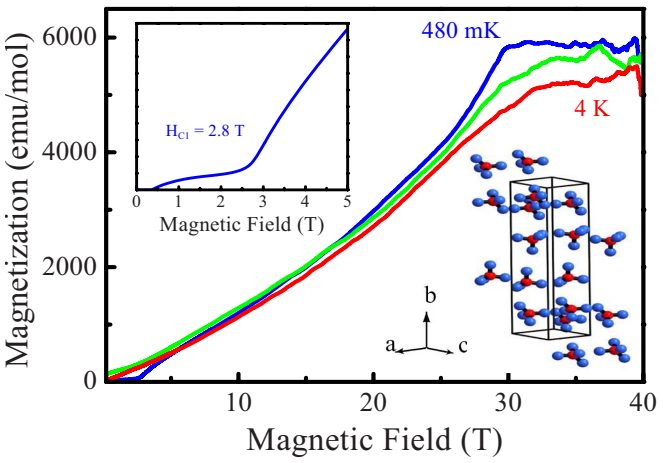

FIG. 1. (Color online) Magnetization of $(2,3\text{-dmpyH})_2CuBr_4$ at 4.0 K, 1.6 K, and 480 mK for $H \| b$. The 480 mK data show H_{c1} and H_{c2} most clearly. Upper inset: closeup view of H_{c1}. Lower inset: 300 K structure of $(2,3\text{-dmpyH})_2CuBr_4$ (Ref. 6). The organic counterions are omitted for clarity.

quantify optical contrast as a function of field. Spin densities were calculated using the Vienna *ab initio* simulation package[23–25] with the generalized-gradient approximation,[26] the plane-wave cutoff energy of 400 eV, and 50 k-points for the irreducible Brillouin zone. $U_{eff}=4$ eV was employed for the Cu $3d$ states.[27]

Theoretical values of $\mu_0 H_{c1}$ and $\mu_0 H_{c2}$ were estimated in advance of our magnetization experiments using two different models[28,29] along with Shapiro's values of the exchange interactions and singlet-triplet spin gap ($J_{\|}=-16.8$ K, $J_{\perp}=-8.68$ K, $\Delta=3.69$ K).[6,29] Together, these models predict critical fields of 2.52 T ($\mu_0 H_{c1}$) and 29.7 T ($\mu_0 H_{c2}$) (Table I). Because the Greven model was developed under strong-rung conditions, it is not perfectly suited for our strong rail system. Nevertheless, estimates of the important magnetic energy scales are in excellent agreement with the experimental data (discussed below), indicating that the model can, to a certain extent, be extrapolated outside the formal range of its validity.

Figure 1 displays the magnetization of $(2,3\text{-dmpyH})_2CuBr_4$ as a function of applied field. The 480 mK results reveal that $\mu_0 H_{c1}=2.8$ T, $\mu_0 H_{c2}=29.0$ T, and $M_{sat}=5700$ emu/mol. Here, $\mu_0 H_{c1}$ is the energy scale of spin-gap closure. Between $\mu_0 H_{c1}$ and $\mu_0 H_{c2}$, the spins cant toward the field, finally reaching the fully polarized state at $\mu_0 H_{c2}$. The overall upward curvature is due to quenching of quantum moments by the field, an effect that is most easily observed in low-dimensional systems.[13] The Greven and de Jongh models (Table I) are in good agreement with our experimental results for the critical fields.[28,29] Reevaluating the expression for the singlet-triplet spin gap ($\Delta=\mu_B g H_{c1}$) using our measured value of $\mu_0 H_{c1}$ and the spectroscopic g factor for $H \| b$, we find $\Delta=4.0$ K, which compares well with Shapiro's estimate of 3.69 K.[6]

Figure 2(a) displays the low-temperature optical absorption of $(2,3\text{-dmpyH})_2CuBr_4$. The observed excitations were assigned according to electronic-structure calculations of the $CuBr_4^{2-}$ chromophore,[17] which indicate that the majority of

TABLE I. Theoretical predictions of magnetic energy scales using two different models assuming $g=2.12$. Experimentally, we find $\mu_0 H_{c1}=2.8$ T, $\mu_0 H_{c2}=29.0$ T, and $\Delta=4.0$ K.

Model	Equation	Theoretical estimates
Greven[a]	$\Delta=0.41\|J_{\perp}\|$	$\Delta=3.56$ K
		$\mu_0 H_{c1}=2.52$ T
de Jongh[b]	$g\mu_B H_{c2}=[2\|J_{\|}\|+\|J_{\perp}\|]k_B$	$\mu_0 H_{c2}=29.7$ T

[a]Reference 28. [b]Reference 29.

features are d to d in nature [Fig. 2(b)]. The low-energy peaks at ~0.6 and 1.0 eV are assigned as combined $4B_2 \rightarrow 6A_1$ and $5A_1 \rightarrow 6A_1$ excitations along the a and c directions, respectively. The trio of peaks at ~1.91, 2.13, and 2.34 eV is assigned to combinations of $3B_1$, $3B_2$, $4A_1 \rightarrow 6A_1$ and $2B_1$, $2B_2$, $3A_1 \rightarrow 6A_1$ transitions. The broad peak centered at ~3.5 eV is assigned as a combination of $1B_1$, $1B_2$, $2A_1 \rightarrow 6A_1$, and $1A_1 \rightarrow 6A_1$ excitations. Here, the $6A_1$ final state consists of a Cu x^2-y^2-orbital plus the Br $4s$ and the Br $4p$ orbitals in an antibonding combination. Higher-energy features were not considered in the model calculation, although they are probably related to excitations from filled s orbitals to the highest-occupied molecular orbital and/or charge transfer between organic cations and $CuBr_4^{2-}$ anions.

Figure 2(c) displays a closeup view of the magneto-optical response of $(2,3\text{-dmpyH})_2CuBr_4$ between 0 and 53 T. With increasing field, we observe small changes in the trio of peaks centered at 2.2 eV and a systematic intensity reduction between 2.4 and 2.8 eV, where the $1B_1 \rightarrow 6A_1$ and $1B_2 \rightarrow 6A_1$ excitations are expected to occur. The field-induced change in absorption in the 2.4–2.8 eV range is substantial and cannot be explained by simple g factor or Zeeman-splitting arguments. Our complementary electron-paramagnetic-resonance results (not shown) indicate that g varies between 2.08 and 2.27 depending on temperature and orientation.[30] Taking $g=2.12$ and Zeeman splitting that goes as $\mu_B g H$, we estimate a slope of $\approx 1.23 \times 10^{-4}$ eV/T, which yields 6.5×10^{-3} eV at 53 T. The Zeeman energy is clearly small compared to the field-induced color property changes in the ~2.4–2.8 eV regime. Combined with the lack of a derivativelike signature in the absorption difference data, this result argues against mechanisms based on simple Zeeman splitting of electronic levels. Field-induced color changes have been observed in other materials[17,31–38] and attributed to the interplay between charge, structure, and magnetism. As discussed below, we attribute the magnetochromic response in $(2,3\text{-dmpyH})_2CuBr_4$ to charge-spin coupling.

Field-induced spectral modifications can be difficult to discern in the absolute absorption spectrum so it is common to calculate the absorption difference $\alpha(E,H)-\alpha(E,0)$ to emphasize changes in the optical properties. The inset of Fig. 2(c) displays the absolute value of the absorption difference of $(2,3\text{-dmpyH})_2CuBr_4$.[39] This rendering highlights the aforementioned magnetic field-induced modifications in the band edge and the trio of peaks centered at 2.2 eV, the latter of which is difficult to see in the main panel. We quantify these effects by integrating the absolute absorption difference spectra and plotting the results as a function of applied mag-

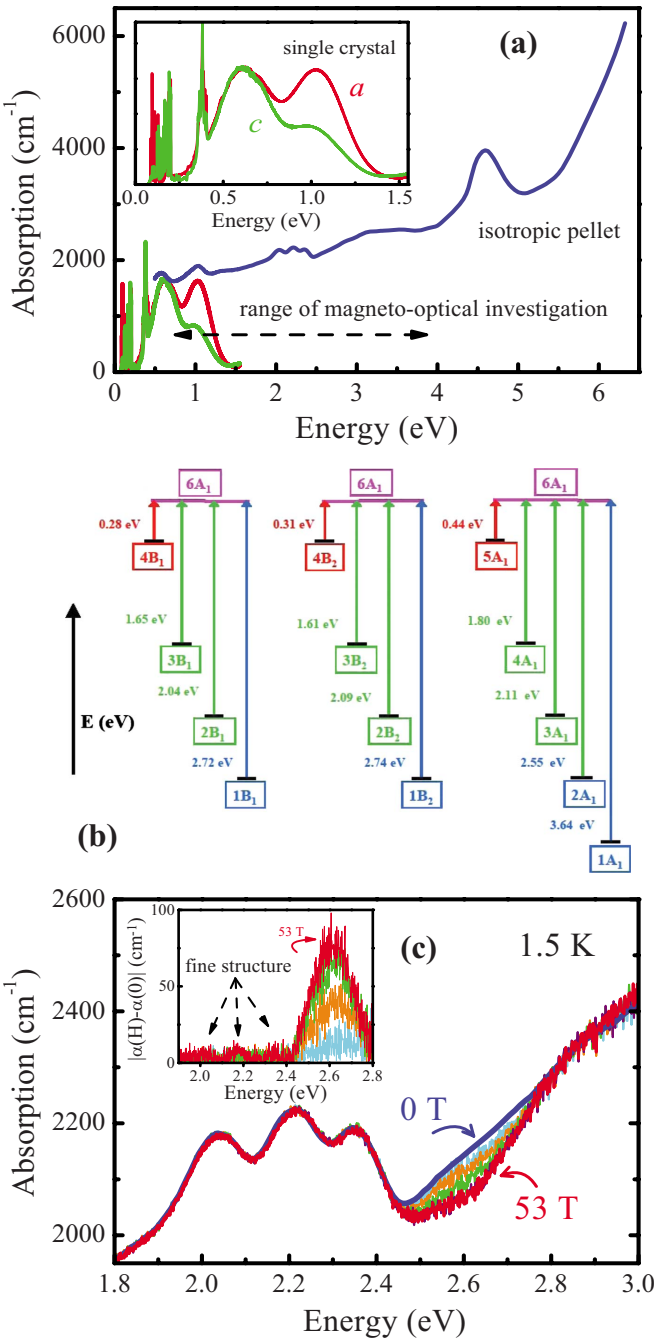

FIG. 2. (Color online) (a) Absorption of $(2,3\text{-dmpyH})_2CuBr_4$ in single-crystal and isotropic pellet forms. Inset: closeup view of single-crystal data showing the polarization dependence. The black dashed arrow indicates the range of our magneto-optical investigation. (b) Schematic view of the d manifold excitations of $CuBr_4^{2-}$ from Ref. 17. (c) Low-temperature magneto-optical response at 0, 20, 23, 27, 35, and 53 T. Inset: closeup view of the absolute value of the absorption difference spectra at the same fields (20, 23, 27, 35, and 53 T).

netic field [Fig. 3(a)]. Strikingly, optical contrast tracks the magnetization. Although an $\mu_0 H_{c1}$-like energy scale is not obvious in the data (likely due to sensitivity issues), the optical contrast grows between $\mu_0 H_{c1}$ and $\mu_0 H_{c2}$ (more slowly than magnetization between 0 and 18 T and superlinearly as

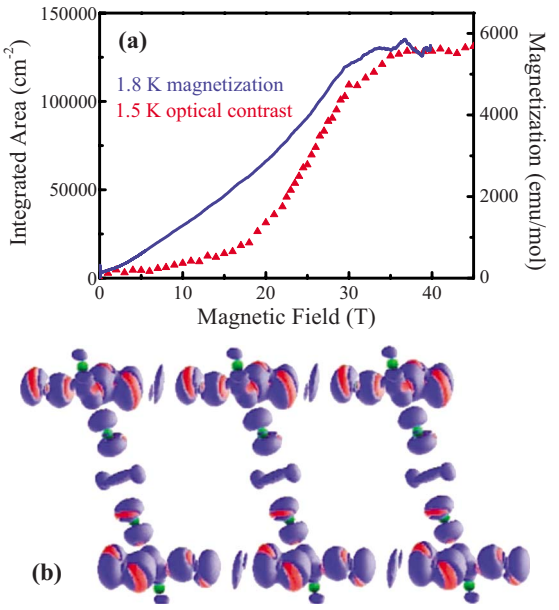

FIG. 3. (Color online) (a) Low-temperature magnetization of $(2,3\text{-dmpyH})_2CuBr_4$ compared with the magneto-optical contrast. (b) Spin-density distribution difference $\Delta\rho=\rho_{AFM}-\rho_{FM}$, where ρ_{AFM} and ρ_{FM} are the calculated spin-density distributions of the AFM and FM states of $(2,3\text{-dmpyH})_2CuBr_4$. The region of blue (darker) [red (lighter)] color indicates that the FM state has a higher (lower) density than the AFM state.

the magnetization approaches saturation), and it saturates along with magnetization in the fully polarized magnetic state. No hysteresis was observed.[40] The optical properties are sensitive to the field-driven transition to the fully polarized state, which demonstrates that the magnetic transition does not take place in isolation.

We also evaluated lattice effects. Complementary magneto-infrared measurements (not shown) do not, however, show any local structure changes within our sensitivity. This is different from other low-dimensional copper halides studied by our team,[18] demonstrating that lattice degrees of freedom do not participate in all magnetically-driven transitions.

To gain insight into the origin of the observed field-induced color change in $(2,3\text{-dmpyH})_2CuBr_4$, we examined the spin-density distribution in the antiferromagnetic (AFM) and fully polarized (FM) states, ρ_{AFM} and ρ_{FM}, respectively. To emphasize small differences between ρ_{AFM} and ρ_{FM}, we calculated the density difference $\Delta\rho=\rho_{AFM}-\rho_{FM}$ [Fig. 3(b)]. The spin density of a $CuBr_4^{2-}$ unit derives from the $6A_1$ magnetic orbital to which each Br center contributes $4s$ and $4p$ character. Our calculations show that the $4p$-orbital contribution from each Br atom is stronger in the FM state than in the AFM state. This is particularly so for the rail-directed Cu-Br bonds. The normalization condition requires a concomitant reduction in the $4s$-orbital contribution from each Br center in the FM state compared to that in the AFM state. Thus, with increasing magnetic field, the character of the $6A_1$ orbital in each $CuBr_4^{2-}$ unit changes such that the Br $4p$-orbital contribution increases and the Br $4s$-orbital contribution decreases. This modification of orbital character is highlighted in the $\Delta\rho$ plot of Fig. 3(b). The magnetic overlap of these

molecular units also depends upon the state. Better overlap is found at high field. In the FM (AFM) state, the $6A_1$ orbitals of $CuBr_4^{2-}$ chromophores combine to yield no node (a node) in the spin-density distribution between adjacent $CuBr_4^{2-}$ units.

The field-induced change in orbital character has important consequences for the transition dipole moments $\langle 1B_1|e\vec{r}|6A_1\rangle$ and $\langle 1B_2|e\vec{r}|6A_1\rangle$. Given the local nature of the excitations, the relevant atomic-orbital contributions to these matrix elements are the $\langle 4p(1B_1 \text{ or } 1B_2)|e\vec{r}|4s(6A_1)\rangle$ terms at each Br center. A field-induced decrease in the Br 4*s*-orbital contribution in the $6A_1$ orbital will decrease the matrix elements of $1B_1 \rightarrow 6A_1$ and $1B_2 \rightarrow 6A_1$ excitations, in line with the observed field-induced reduction in absorption intensity in the 2.4–2.8 eV region.

To summarize, we investigated the magnetic and optical properties of $(2,3\text{-dmpyH})_2CuBr_4$, an antiferromagnetic quantum spin ladder with strong rail interactions. Despite the large difference between the magnetic and electronic energy scales, there is substantial coupling between the spin and charge channels. This coupling gives rise to a field-induced change in the optical properties. In $(2,3\text{-dmpyH})_2CuBr_4$, the optical contrast tracks the magnetization because the Br 4*s*-orbital contribution to the empty down-spin band, into which the optical excitations take place, depends on the spin arrangement between adjacent $CuBr_4^{2-}$ chromophores. This mechanism may be important for understanding magnetochromism in other molecule-based materials. Indeed, the consequence of nodal vs non-nodal patterns in the spin-density distribution is an emerging theme that explains coupling in many molecular systems[18] and can be exploited to achieve color contrast in other materials.

This work is supported by the DMR NSF (UT, Clark, NHMFL), MSD DOE and Science in 100 T program (NCSU, ORNL, and NHMFL), and the State of Florida (NHMFL).

[1] A. Gozar, G. Blumberg, B. S. Dennis, B. S. Shastry, N. Motoyama, H. Eisaki, and S. Uchida, Phys. Rev. Lett. **87**, 197202 (2001).
[2] V. V. Moshchalkov, L. Trappeniers, and J. Vanacken, Europhys. Lett. **46**, 75 (1999).
[3] M. Azuma, Z. Hiroi, M. Takano, K. Ishida, and Y. Kitaoka, Phys. Rev. Lett. **73**, 3463 (1994).
[4] X. Ribas *et al.*, Adv. Funct. Mater. **15**, 1023 (2005).
[5] F. Xiao *et al.*, Phys. Rev. B **79**, 134412 (2009).
[6] A. Shapiro *et al.*, J. Am. Chem. Soc. **129**, 952 (2007).
[7] R. D. Willett *et al.*, Inorg. Chem. **43**, 3804 (2004).
[8] F. Awwadi *et al.*, Inorg. Chem. **47**, 9327 (2008).
[9] P. R. Hammar, D. H. Reich, C. Broholm, and F. Trouw, Phys. Rev. B **57**, 7846 (1998).
[10] B. Lake *et al.*, Nature Mater. **4**, 329 (2005).
[11] B. C. Watson, V. N. Kotov, M. W. Meisel, D. W. Hall, G. E. Granroth, W. T. Montfrooij, S. E. Nagler, D. A. Jensen, R. Backov, M. A. Petruska, G. E. Fanucci, and D. R. Talham, Phys. Rev. Lett. **86**, 5168 (2001).
[12] C. P. Landee *et al.*, Polyhedron **22**, 2325 (2003).
[13] P. A. Goddard *et al.*, New J. Phys. **10**, 083025 (2008).
[14] M. G. Banks, R. K. Kremer, C. Hoch, A. Simon, B. Ouladdiaf, J.-M. Broto, H. Rakoto, C. Lee, and M.-H. Whangbo, Phys. Rev. B **80**, 024404 (2009).
[15] N. A. Fortune, S. T. Hannahs, Y. Yoshida, T. E. Sherline, T. Ono, H. Tanaka, and Y. Takano, Phys. Rev. Lett. **102**, 257201 (2009).
[16] M. B. Stone, W. Tian, M. D. Lumsden, G. E. Granroth, D. Mandrus, J.-H. Chung, N. Harrison, and S. E. Nagler, Phys. Rev. Lett. **99**, 087204 (2007).
[17] J. D. Woodward, J. Choi, J. L. Musfeldt, J. T. Haraldsen, X. Wei, H.-J. Koo, D. Dai, M.-H. Whangbo, C. P. Landee, and M. M. Turnbull, Phys. Rev. B **71**, 174416 (2005).
[18] J. L. Musfeldt, L. I. Vergara, T. V. Brinzari, C. Lee, L. C. Tung, J. Kang, Y. J. Wang, J. A. Schlueter, J. L. Manson, and M.-H. Whangbo, Phys. Rev. Lett. **103**, 157401 (2009).
[19] O. Sato *et al.*, Inorg. Chem. **38**, 4405 (1999).
[20] D. A. Pejaković, J. L. Manson, J. S. Miller, and A. J. Epstein, Phys. Rev. Lett. **85**, 1994 (2000).
[21] C. Broholm (unpublished).
[22] For some experiments, crystals were mixed with dry, optically transparent KCl powder to prepare isotropic pellet samples.
[23] P. E. Blöchl, Phys. Rev. B **50**, 17953 (1994).
[24] G. Kresse and D. Joubert, Phys. Rev. B **59**, 1758 (1999).
[25] G. Kresse and J. Furthmüller, Phys. Rev. B **54**, 11169 (1996).
[26] J. P. Perdew, K. Burke, and M. Ernzerhof, Phys. Rev. Lett. **77**, 3865 (1996).
[27] S. L. Dudarev, G. A. Botton, S. Y. Savrasov, C. J. Humphreys, and A. P. Sutton, Phys. Rev. B **57**, 1505 (1998).
[28] M. Greven, R. J. Birgeneau, and U.-J. Wiese, Phys. Rev. Lett. **77**, 1865 (1996).
[29] L. J. de Jongh, A. R. Miedema, Adv. Phys. **23**, 1 (1974); **50**, 947 (2001).
[30] R. D. McDonald (unpublished).
[31] J. Choi, J. D. Woodward, J. L. Musfeldt, X. Wei, M.-H. Whangbo, J. He, R. Jin, and D. Mandrus, Phys. Rev. B **70**, 085107 (2004).
[32] J. H. Jung, H. J. Lee, T. W. Noh, Y. Moritomo, Y. J. Wang, and X. Wei, Phys. Rev. B **62**, 8634 (2000).
[33] J. H. Jung, H. J. Lee, T. W. Noh, E. J. Choi, Y. Moritomo, Y. J. Wang, and X. Wei, Phys. Rev. B **62**, 481 (2000).
[34] Y. Okimoto, Y. Tomioka, Y. Onose, Y. Otsuka, and Y. Tokura, Phys. Rev. B **59**, 7401 (1999).
[35] P. J. McCarthy and H. U. Guedel, Inorg. Chem. **23**, 880 (1984).
[36] C. Bellitto, T. E. Wood, and P. Day, Inorg. Chem. **24**, 558 (1985).
[37] X. S. Xu *et al.*, Phys. Rev. Lett. **101**, 227602 (2008).
[38] E. Kojima *et al.*, Phys. Rev. B **77**, 212408 (2008).
[39] The absolute value quantifies total optical contrast.
[40] The short-pulse duration offers limited control over pulse shape and rise time, precluding sweep-rate studies in which the rate varies over several orders of magnitude.